

AD/A-0 480

PROTECTION OF THE CARDIOPULMONARY
SYSTEMS AGAINST THE INJURIOUS EFFECTS
OF ACCELERATION

Earl H. Wood, et al

Mayo Foundation

Prepared for:

Air Force Office of Scientific Research

1974

DISTRIBUTED BY:

NTIS

National Technical Information Service
U. S. DEPARTMENT OF COMMERCE

UNCLASSIFIED

SECURITY CLASSIFICATION OF THIS PAGE (When Data Entered)

REPORT DOCUMENTATION PAGE		READ INSTRUCTIONS BEFORE COMPLETING FORM	
1. REPORT NUMBER AFOSR - TR - 74 - 1622	2. GOVT ACCESSION NO.	3. RECIPIENT'S CATALOG NUMBER ADA-000480	
4. TITLE (and Subtitle) PROTECTION OF THE CARDIOPULMONARY SYSTEMS AGAINST THE INJURIOUS EFFECTS OF ACCELERATION		5. TYPE OF REPORT & PERIOD COVERED Interim 1 July 1973 - 30 June 1974	
7. AUTHOR(s) Earl H. Wood, James F. Greenleaf, Peter A. Chevalier		6. PERFORMING ORG. REPORT NUMBER	
9. PERFORMING ORGANIZATION NAME AND ADDRESS Mayo Foundation Department of Physiology and Biophysics Rochester, Minnesota 55901		8. CONTRACT OR GRANT NUMBER(s) F44620-71-C-0069	
11. CONTROLLING OFFICE NAME AND ADDRESS Air Force Office of Scientific Research (NL) 1400 Wilson Boulevard Arlington, Virginia 22209		10. PROGRAM ELEMENT, PROJECT TASK AREA & WORK UNIT NUMBERS 9777/61102F/681312	
14. MONITORING AGENCY NAME & ADDRESS (if different from Controlling Office)		12. REPORT DATE -- 1974	
		13. NUMBER OF PAGES 25	
		15. SECURITY CLASS. (of this report) UNCLASSIFIED	
		15a. DECLASSIFICATION/DOWNGRADING SCHEDULE	
16. DISTRIBUTION STATEMENT (of this Report) Approved for public release; distribution unlimited.			
17. DISTRIBUTION STATEMENT (of the abstract entered in Block 20, if different from Report)			
18. SUPPLEMENTARY NOTES			
19. KEY WORDS (Continue on reverse side if necessary and identify by block number) Reproduced by NATIONAL TECHNICAL INFORMATION SERVICE U S Department of Commerce Springfield VA 22151			
20. ABSTRACT (Continue on reverse side if necessary and identify by block number) The annual report gives a brief summary of individual studies and activities performed during the past year. Progress accomplished centered primarily on application of recently developed techniques to the study of the spatial distribution of strains and ventilation within the lung parenchyma. It is clear that the parenchymal marker and three-dimensional reconstruction techniques described will add significant new information to understanding of dynamic regional stress-strain relationships throughout the lung and will provide the			

DD FORM 1473
1 JAN 73

EDITION OF 1 NOV 65 IS OBSOLETE

UNCLASSIFIED

SECURITY CLASSIFICATION OF THIS PAGE (When Data Entered)

UNCLASSIFIED

SECURITY CLASSIFICATION OF THIS PAGE(When Data Entered)

20. ABSTRACT - continued.

methodology to study the effects on regional lung function of alterations in these parameters induced by changes in the gravitational-inertial force environment.

ii

UNCLASSIFIED

SECURITY CLASSIFICATION OF THIS PAGE(When Data Entered)

Annual Progress Report (July 1, 1973 - June 30, 1974)

Contract No. F44620-71-C-0069

Purchase Request No. 74-007

PROTECTION OF THE CARDIOPULMONARY SYSTEMS AGAINST THE
INJURIOUS EFFECTS OF ACCELERATION

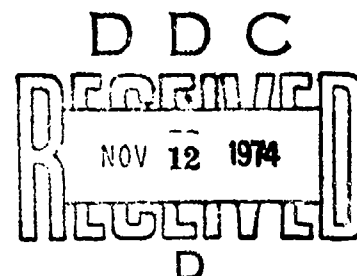
Evaluation of effects of time history of gravitational-inertial force environment on regional dynamic distribution of pulmonary ventilation, strains, edema and blood volume.

This report gives a brief summary of individual studies and activities performed during the period July 1, 1973 to June 30, 1974. Progress accomplished during the period centered primarily on the application of recently developed techniques to the study of the spatial distribution of strains and ventilation within the lung parenchyma.

1. Regional Distribution of Strain Within the Lung
Parenchyma from Measurements of the Dynamic
Displacement of Metallic Parenchymal Markers

In order to assess regional lung mechanics under dynamic conditions, measurements of high spatial resolution must be obtained of the distribution of regional parenchymal strains with simultaneous measurements of regional transpulmonary pressures as well as related intravascular pressures. The spatial distribution of pulmonary parenchymal strains and changes in regional volumes in the intact thorax of the dog were determined utilizing the pulmonary parenchymal marker technique. This technique involves tagging the pulmonary parenchyma of the right lung with 20-30 1-mm diameter metallic

-1-
Approved for public release;
distribution unlimited.



markers which are implanted percutaneously under fluoroscopic control 2-3 weeks prior to the study (1). Post-mortem studies have demonstrated that there is no significant pleural reaction following implantation of the markers and pulmonary parenchymal pathologic changes are limited to within 100-200 micra surrounding each marker.

Experimentally, 14 kg dogs were suspended head-up or head-down in a water-immersion respirator (Figure 1) with the animal's airway connected to ambient air. The important advantage of the water-immersion respirator lies in its ability to provide accurate and reproducible control of lung volumes and respiratory rate, while end-expiratory volume can be selectively altered and controlled by adding or subtracting fluid from the constant volume system.

IMMERSION RESPIRATOR

Dynamic Spatial Reconstruction of Canine Thorax and Contents

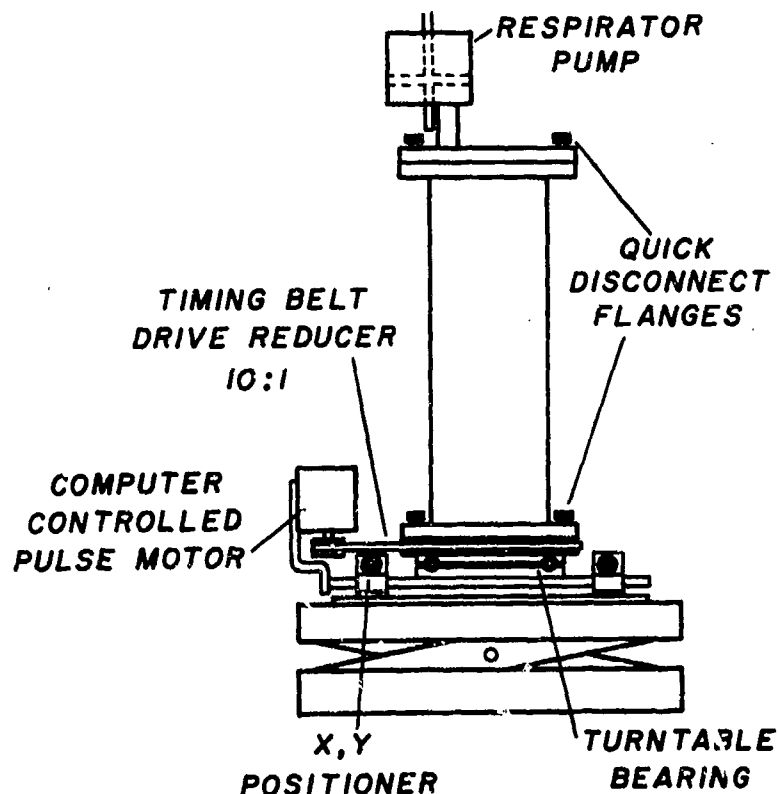


Figure 1. Schematic design of computer-controlled water-immersion respirator. Dog is supported upright in a cylindrical container filled with water. Removal and addition of water from and to the container by a respirator pump provides accurate control of respiratory rate, tidal, and residual volumes. This assembly consists of a position control which directs movement of the cylinder either vertically or horizontally with respect to the image intensifier, a belt-driven turntable for rotating the cylinder, and an incremental stepping motor controlled by signals from the computer and attached to the driving belt to accomplish rotation of the turntable. This system provides:
1) accurately reproducible computer-controlled respiratory cycles throughout the period

in which the video roentgen views are recorded; 2) constant temporal relationships between successive heart beats and the respiratory cycle by computer-control of cardiac pacing and respiratory rate; 3) capability of studying cardiac and pulmonary function with various permutations of respiratory rate, tidal and residual volumes and detailed analysis of individual heart beats at any phase of the respiratory cycle.

The water surrounding the dog also provides an ideal hydrostatic pressure environment for support of the dog's vascular system while in the vertical, head-up position. The vertical position is required so that the dog's body position in relation to gravity is constant so that gravitational-induced shifts in the relative positions of intrathoracic and abdominal organs do not occur.

Furthermore, the water provides a constant background roentgen absorption similar to that of body tissue. The resulting nearly constant transmission characteristics in effect maintains a more nearly exponential relationship (Beer's law) between transmitted radiation and attenuation of the incident roentgen beam in spite of its non-monochromatic nature. This also facilitates calibration of x-ray absorption values and by reducing the maximum gray scale range in the recorded image, allows attainment of maximal sensitivity for detection and three-dimensional mapping of roentgen density variations within the animal's body.

In addition, because of the constant x-ray path length across the water-filled cylindric respirator, changes in roentgen density at any site over the lung fields will be a function of changes in amount of air being transradiated at this site. Consequently, the instant-to-instant spatial distribution of ventilation can be measured throughout the respiratory cycle.

The dynamic displacements of the parenchymal markers during various respiratory maneuvers are measured by means of the stereo biplane videoroentgenographic system and recording equipment shown in Figure 2. Two x-ray sources transilluminate the thorax and the fluoroscopic images are recorded on the two image intensifiers. The stereo biplane videoroentgenograms are combined into a single biplane video format (Figure 3) and recorded on videotape in absolute temporal synchrony with up to 16 channels of analog information, such as intrathoracic pressures, ECG, and ventilation (2).

DYNAMIC REGIONAL LUNG MECHANICS

Stereo Video Roentgenographic Analysis

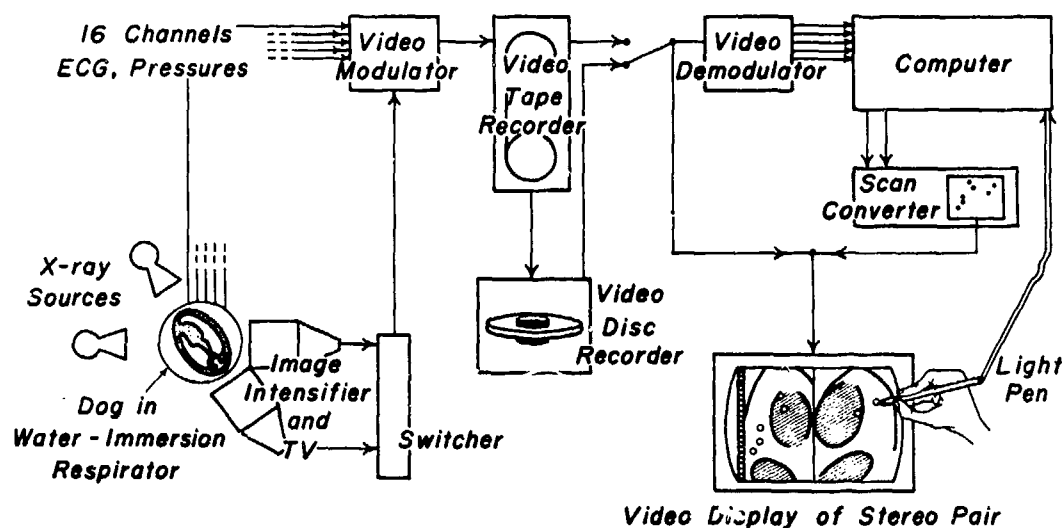


Figure 2. Schematic drawing of stereo biplane video-roentgenographic system used to study dynamic regional lung mechanics. Dog is suspended head-up or head-down in the water-immersion respirator. Sixteen channels of analog information are recorded in absolute temporal synchrony with the video image on the videotape. Subsequent analysis is performed after transferring the video and analog information to stop-action video disc. An operator-interactive computer program is used to input the geometric coordinates of the metallic parenchymal markers into the computer where the true spatial coordinates are determined after correction for pin-cushion and magnification distortions.

For analysis, the biplane images plus multichannel analog recordings are transferred from videotape to stop-action video disc, and the tracking of the geometric positions of the metallic markers is performed with the aid of an operator-interactive

computer program. A video scan converter produces a computer-generated cursor which is superimposed on the stop-action display of the biplane thoracic image. The investigator moves this cursor until it coincides with one of the metallic markers at which time the investigator depresses a key on the keyboard to interrupt the computer and the geometric coordinates of the cursor and thus the metallic markers are input and stored in an array. This procedure is repeated until the geometric coordinates of all identifiable markers on both projections of the lungs for a single video frame are input into the computer. Simultaneously, the computer digitizes the 16 channels of analog data which had been recorded simultaneously with the video information. The true spatial coordinates of each marker corrected for pin-cushion and magnification distortions are then determined.

An example of a video frame used for such analysis is shown in Figure 3.

**STEREO BIPLANE END-INSPIRATORY VIDEO
ROENTGENOGRAM FOR MEASUREMENT OF SPATIAL
POSITION OF PARENCHYMAL TAGS IN RIGHT LUNG**



Figure 3. Photograph of single frame of stereo biplane videoroentgenogram illustrating the stereo biplane view of the canine lung with metallic parenchymal markers in

the right lung and the cursor dots used to input the geometric positions of the markers shown in the right-hand image. Sixteen channels of analog data (pressures and ECG) recorded in absolute temporal synchrony with the video image are contained in the "ribbon" at the left border of the image. Identifying information, e.g., time and code, added during the course of the experiment is displayed at the bottom of the image.

The simultaneously-recorded analog information is contained in the "ribbon" at the left-hand margin of the photo while identification information (e.g., time and code), added during the experiment, is displayed at the bottom of the photo. In this particular photograph the geometric positions of the metallic markers at end-expiration are indicated by the cursor dots in the right-hand panel of this biplane thoracic image. Subsequently, the stop-action video disc was stepped forward to end-inspiration and this photograph was taken. By comparing the positions of the markers at end-expiration indicated by the cursor dots and end-inspiration indicated by the markers themselves, a qualitative measure of the direction and magnitude of parenchymal displacement occurring during one respiratory cycle is obtained.

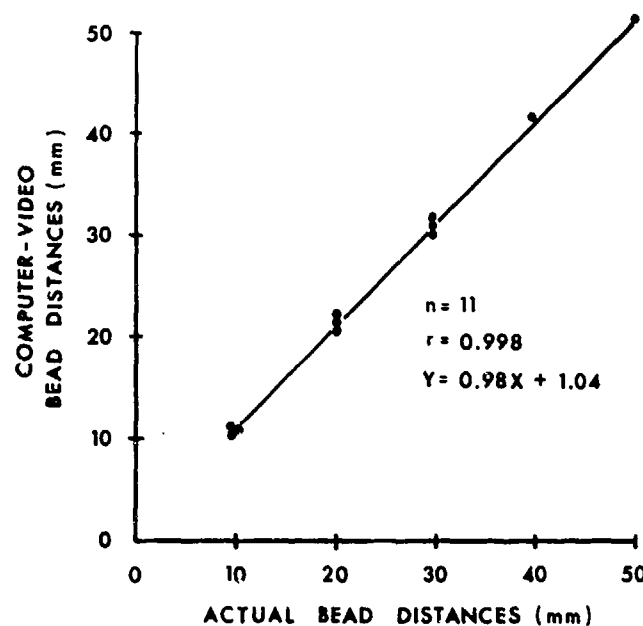


Figure 4. Comparison of actual and computer-calculated distances between pairs of radiopaque markers fixed at

known distances within a lucite plate and transradiated by orthogonal biplane x-ray system. Markers positions on video image were identified with the cursor and their geometric coordinates stored in an array. Distances between markers were computer determined after removal of magnification and pin-cushion distortions.

The accuracy of this technique is indicated in Figure 4 which compares the actual measured distances between markers imbedded in a lucite plate which was rotated in the biplane x-ray system and the computer-determined distances obtained from the videoroentgenographic images. This graph indicates that the computer analysis which removes pin-cushion and magnification distortions is accurate to within a few millimeters.

Actual results from the computer program which calculates the geometric coordinates of the individual markers in three-dimensional space are shown in Figure 5.

**DIRECTION AND MAGNITUDE OF PARENCHYMAL
DISPLACEMENT DURING RESPIRATORY CYCLE**
(Dog, 14 kg, Morphine - Pentobarbital Anesthesia,
Water-Immersion Respirator,
Head-Up, 12 breaths/minute)

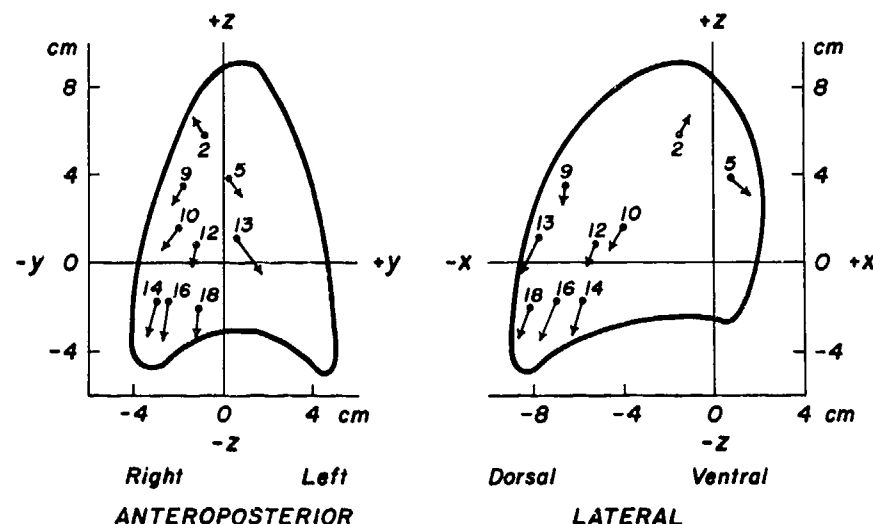


Figure 5. Comparison of regional displacements from FRC of metallic parenchymal markers in the right lung during a respiratory cycle. Positions of the individual markers

at end-expiration and end-inspiration are indicated by the tail and the head of each arrow, respectively. Orientation and length of each arrow denotes direction and magnitude, respectively, of regional parenchymal displacement. Dog was suspended head-up in the water-immersion respirator.

The spatial locus of each marker can be found by looking at the anteroposterior (left-hand panel) and lateral (right-hand panel) projections of the lung. The tail of the individual arrows represent the position of the marker at end-expiration while the head of the arrow represents the position of each individual marker at end-inspiration. Thus, the arrows indicate the direction and magnitude of regional parenchymal displacements during a respiratory cycle. Clearly, analysis of the dynamic displacements of these metallic parenchymal markers can be used to determine the distribution of regional strains within the lung of the intact thorax during various respiratory maneuvers and under different gravitational-inertial force environments.

Figure 6 indicates the positions of 3 pairs of markers at functional residual capacity (FRC).

**POSITIONS OF MARKER PAIRS AT FRC FOR STUDY
OF REGIONAL LUNG PARENCHYMAL STRAINS
DURING RESPIRATORY CYCLE**

*(Dog, 14 kg, Morphine-Pentobarbital Anesthesia,
Water-Immersion Respirator,
Head-Up, 12 breaths/minute)*

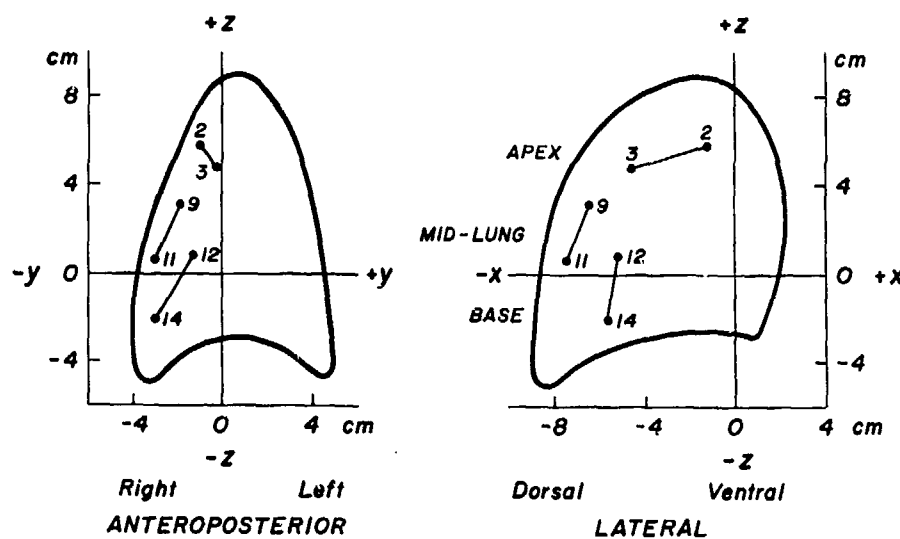


Figure 6. Location and orientation of 3 pairs of markers selected to measure strain in three regions of the lung, i.e., apex, mid-lung, and base.

These pairs of markers were selected for analysis of strain in three regions of the lung, i.e., apex, mid-lung and the base. The dynamic changes in distance in three-dimensional space between each pair of markers represents strain ($\Delta L/L_0$) in that region of the lung for that particular orientation of the marker-pair. Distributions of regional lung parenchymal strains during three respiratory cycles starting at FRC (closed symbols) and three starting at FRC + 200 ml (open symbols) are shown in Figure 7.

REGIONAL LUNG PARENCHYMAL STRAINS DURING THREE
RESPIRATORY CYCLES STARTING AT FRC AND FRC + 200 ml
(Dog, 14 kg, Morphine-Pentobarbital Anesthesia, Water-Immersion
Respirator, Head-Up, 12 breaths / minute)

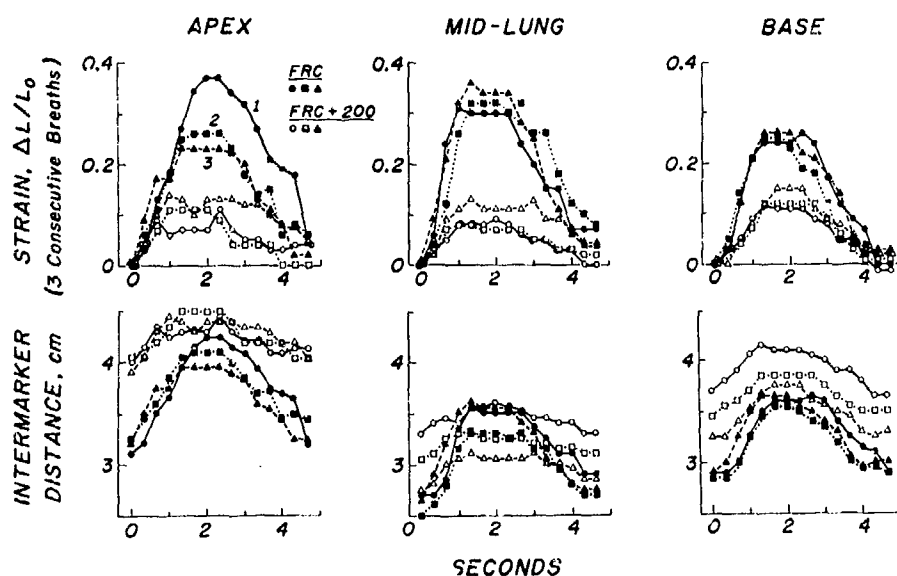


Figure 7. Distributions of regional lung parenchymal strains and displacements during three respiratory cycles starting at FRC (closed symbols) and three respiratory cycles starting at FRC + 200 ml (open symbols). Upper three panels indicate strain distributions for the three pairs of markers in the apex, mid-lung, and base, respectively. Lower three panels represent absolute distance between marker-pairs at the three specified lung levels.

The top three panels indicate strain distributions for the three pairs of beads in the apex, midlung and base, respectively. It can be seen that parenchymal strain was larger at the lower lung volume than at the higher lung volume. The lower three panels represent the absolute distance between the various markers during the respiratory cycle. It is also clear that the absolute distance increased at the higher lung volume; however, the absolute excursion or change in length was less at the higher lung volume than at the lower lung volume. In addition, the excursions at the higher lung volume were more like those at the lower lung volume in the basal region as compared to the apical region of the lung. The reproducibility of the measurements of regional distributions of strain from cycle to cycle can also be seen in this figure.

ANISOTROPY OF PARENCHYMAL STRAINS IN 3 LUNG REGIONS
(Dog, 14 kg, Morphine-Pentobarbital, Anesthesia, Water-Immersion
Respirator, Head-Up, 12 breaths/minute)

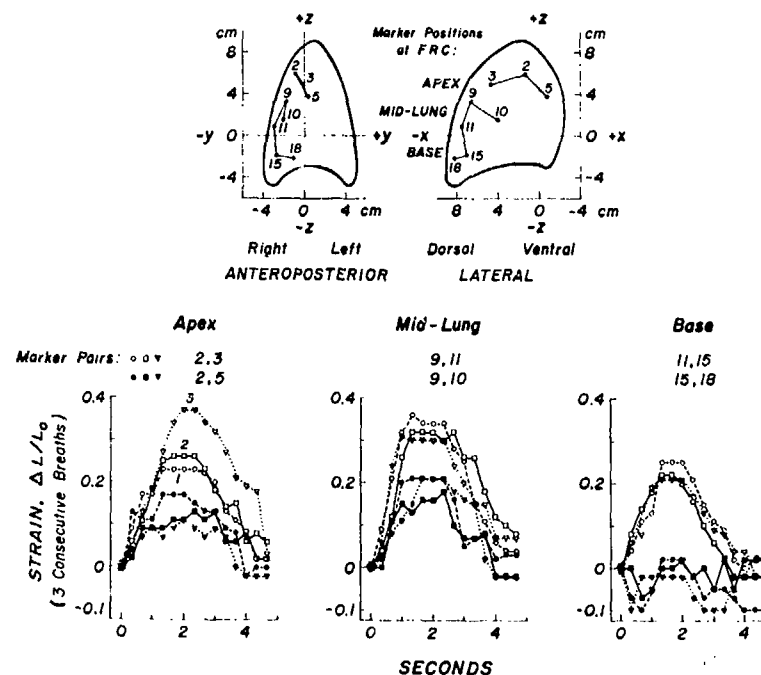


Figure 8. Distribution of parenchymal strains in three different regions of the lung. Upper two panels show location of three sets of 3 markers each chosen to include

in each of three regions, i.e., apex, mid-lung, and base, pairs of markers oriented in virtually orthogonal directions. Lower three panels represent the strains for the pairs of markers in the upper panel. Note the anisotropy of lung expansion at each of the specified lung levels.

The anisotropy of parenchymal strains in three separate lung regions is shown in Figure 8. The upper two panels represent the anteroposterior and the lateral projections of three sets of three markers each. The three sets of markers represent regions in the apex, the midlung and the base and were chosen to include in each region pairs of markers oriented in virtually orthogonal directions. The lower three panels represent the strain for the pairs of markers shown in the upper panel. These three panels represent strains for two marker-pairs in the apex, the midlung and the base, respectively. It can be seen that for three sequential breaths that marker-pairs in both the apex and the midlung regions exhibited different strains depending on their orientation within the lung in their respective regions. It can also be seen that in the base a paradoxical movement is exhibited in that beads 18 and 19 exhibited a decrease in length during inspiration. This behavior has been seen in other parts of the lung as well and was predicted by West and Matthews (3) for the apical region but not for the basal region of the lung of a head-up animal.

Thus far, we have seen in anesthetized-paralyzed dogs in the head-up position in the water-immersion respirator that changes in end-expiratory volume caused varying changes in strain in different regions of the lung and that regional strains are not isotropic. Whether these regional differences in mechanical strain are due to differences in regional stress or to differences in material properties of the lung is not known.

2. Algebraic Reconstruction of Thoracic Cross Sections of the Intact Lungs and Heart of a Living Dog Supported in the Head-up Position in a Water-Immersion Respirator

A new technique for obtaining dynamic three-dimensional images of the thorax and its contents has been described by this laboratory previously (4). This technique provides information concerning the shape and dimensions of the thoracic cavity including the borders of the lung and is based on a mathematical analysis outlined elsewhere (5). The reconstruction of a three-dimensional object through the mathematical analysis of its projection shadows from multiple directions has received an increasing amount of attention recently (6).

We have recently used this technique to determine the distribution of strains in cross sections through the thorax of dogs suspended head-up in a water-immersion respirator and ventilated at constant tidal volume and end-expiratory volume. Cross sections representing the roentgen opacity of transverse sections through the thorax were reconstructed from 35 thoracic videoroentgenograms recorded sequentially at equiangular increments during rotation of the dog through 183.6°. Heart rate and respiration were computer-controlled and synchronized with rotation and with the recording of the image to provide sets of 60/second videoroentgenograms representing the entire anatomic and temporal extent of the cardiac and respiratory cycles when the dog was stationary in each of the 35 positions through the rotation procedure.

Figure 9 illustrates a sequence of cross sections in which the top row is a temporal sequence, from left to right, of three thoracic videoroentgenograms from the same angle of view (approximately a posterior-anterior projection - left side of dog is on left side of roentgenogram) recorded at end-inspiratory,

mid-expiratory and end-expiratory phases of the respiratory cycle, respectively. The left column is a sequence of thoracic videoroentgenograms recorded from the same angle of view at end-inspiration with a brightened horizontal line superimposed on each roentgenogram indicating the level at which the cross-sectional reconstruction of the thorax was obtained. Horizontal bands at the left margin are amplitude modulated recordings of cardiac and respiratory pressures, pacing pulses, and other variables which are recorded simultaneously with the video image information (2).

**PHASIC AND CEPHALOCAUDAL VARIATIONS IN
THORACIC CROSS SECTIONS RECONSTRUCTED FROM
35 MULTIPLANAR ROENTGENOGRAMS OF INTACT DOG
IN WATER-IMMERSION RESPIRATOR**

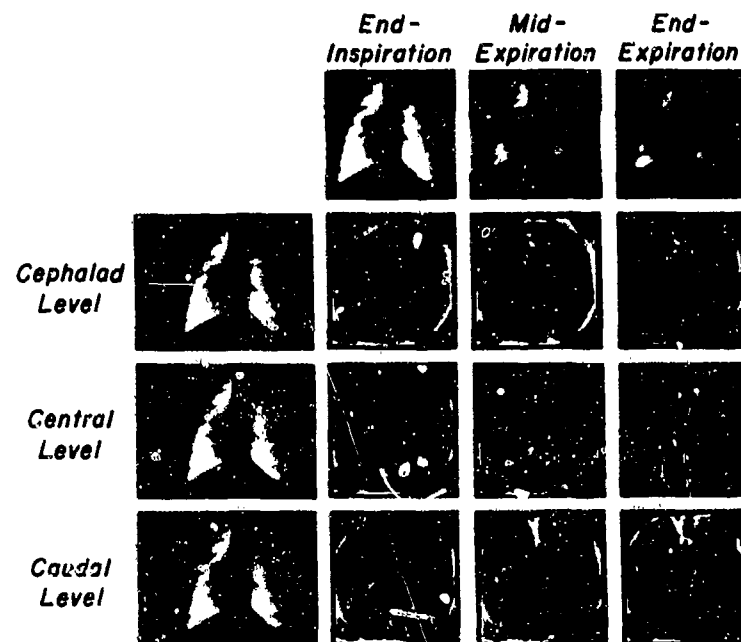


Figure 9. Reconstructed thoracic cross sections of the intact lungs and heart of a living dog supported in the head-up position in a computer-controlled, rotatable, water-immersion respirator. Cross sections were reconstructed from 35 thoracic videoroentgenograms recorded sequentially at equiangular increments during rotation of the dog through 183.6°. Heart rate and respiration were computer controlled and synchronized

with rotation and image recording to provide sets of 60-per-second videoroentgenograms recorded throughout the cardiac and respiratory cycles when the dog was stationary in each of the 35 positions included in the incremental rotational sequence.

Top row is a temporal sequence, from left to right, of three thoracic videoroentgenograms from the same angle of view (approximately a posterior-anterior projection; left side of dog is on left side of roentgenogram) recorded at the end-inspiratory, mid-expiratory and end-expiratory phases of the respiratory cycle, respectively, at which times the reconstructed cross sections in each column were obtained. The left column is a sequence of thoracic videoroentgenograms recorded from the same angle of view at end-inspiration with a brightened horizontal line superposed on each roentgenogram to indicate the three cross-sectional levels of the chest in cephalad to caudad (top-to-bottom spatial) sequence at which the cross-sectional reconstructions in each row were obtained. Horizontal bands at left margin are amplitude modulated recordings of cardiac and respiratory pressures, pacing pulses, and other variables obtained synchronously with video image information.

The rows and columns of reconstructed thoracic cross sections show the anatomical configurations of the lungs and heart at these three different anatomic levels (top-to-bottom) and three different phases of the respiratory cycle (left-to-right) respectively. Dorsal surface of dog is at top and left side is at right of each cross section.

The rows and columns of reconstructed thoracic cross sections show the anatomical configurations of the lung and heart at these three different anatomical levels (top to bottom) and three different phases of the respiratory cycle (left to right) respectively. The dorsal surface of the dog is at the top and the left side is at the right of each cross section.

Note that the margins of the lung and epicardial surfaces of the heart have been reproduced with reasonable fidelity. The bright x-ray dense, white spots within the thorax are the roentgen opaque catheters in the esophagus, heart and inferior

vena cava, respectively. The striking decrease in the cross-sectional areas of the lungs during expiration is evident at the three cephalad-to-caudad and cross-sectional levels of the chest included in this montage. The epicardial surfaces of the heart and the catheter in the right atrium which are visualized in the upper and mid-cross-sectional levels are displaced by the dome of the diaphragm in the basal cross section. The roentgen opaque catheters in the inferior vena cava and esophagus are also visualized in the basal cross sections as the white spots in the mid-dorsal region of the thorax. The cephalad movement of the diaphragm completely displaces the diaphragmatic region of the left lung from the caudad cross-sectional level of the thorax at end-expiration (bottom-right panel).

Using the above described techniques, cross section reconstructions representing five separate levels through the upright thorax of the head-up dog were utilized to calculate the area of the left and right lungs during respiration as a function of time during the respiratory cycle.

Figure 10 represents the change in area of reconstructed cross sections of the intact right and left lung versus time during a respiratory cycle at a respiratory rate of approximately 18 per minute. The brightened horizontal lines on the anteroposterior view of the canine thorax indicate the five levels at which cross sections of the lung were obtained during the respiratory cycle. Plots of changes in relative cross-sectional area (normalized to the maximal cross-sectional area observed - at level 4) versus time are represented, with each plot containing the right (R) and left (L) lung for that particular cross section and lung level. Note the regional differences in cross-sectional area between levels 1 and 4 during the respiratory cycle and at level 5 note that the diaphragm displaces the left lung during approximately half of the respiratory cycle.

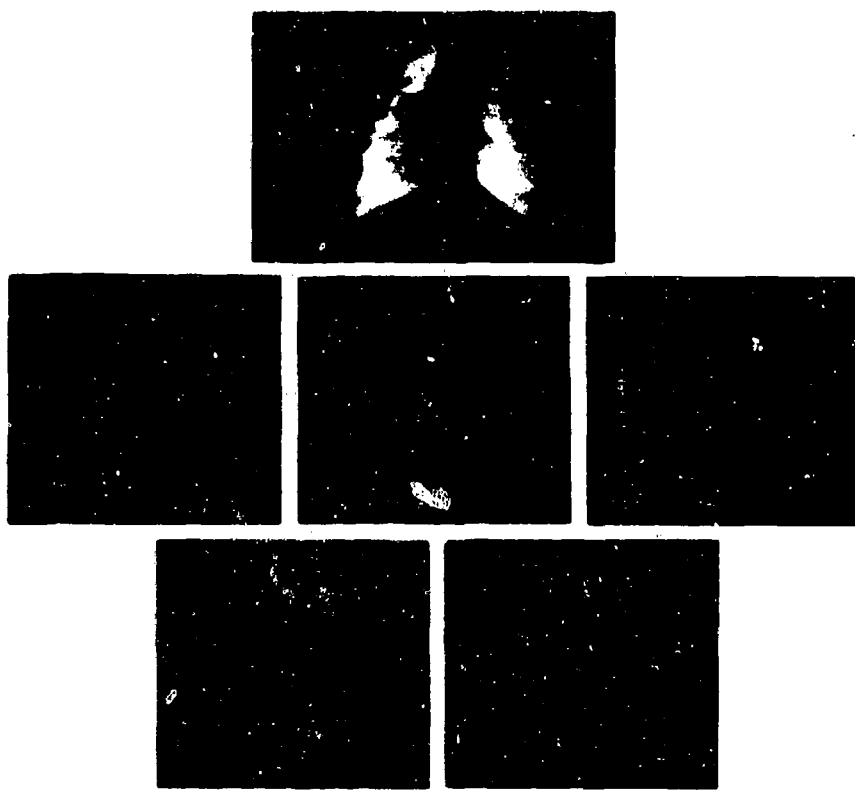


Figure 10. Changes in area of reconstructed cross sections of the intact right and left lung of a living dog at five different levels during the respiratory cycle. Cross sections were reconstructed from 35 thoracic videoroentgenograms recorded sequentially at equiangular increments during rotation of the dog through 183.6° while suspended head-up in a computer-controlled, rotatable, water-immersion respirator. At the center is an anteroposterior view, taken at end-inspiration, of the canine thorax showing a brightened horizontal line for each of the five levels at which cross sections were reconstructed. Around the A-P view are plots of relative cross-sectional area (normalized to the maximal cross-sectional area observed - at level 4) versus time for the right (R) and left (L) lung at each specified lung level. At level 5, the left lung is displaced by the diaphragm during a portion of the respiratory cycle.

The change in regional volume as a function of tidal volume is shown in Figure 11. The cross sections obtained for Figure 10 were used in Figure 11 to determine the change in regional volume (assuming unit thickness for each cross section) as a function of tidal volume (measured from the displacement pump of the water-immersion respirator) at each of the 5 specified levels during the respiratory cycle. The inspiratory (I) and expiratory (E) phases of the respiratory cycle are indicated.

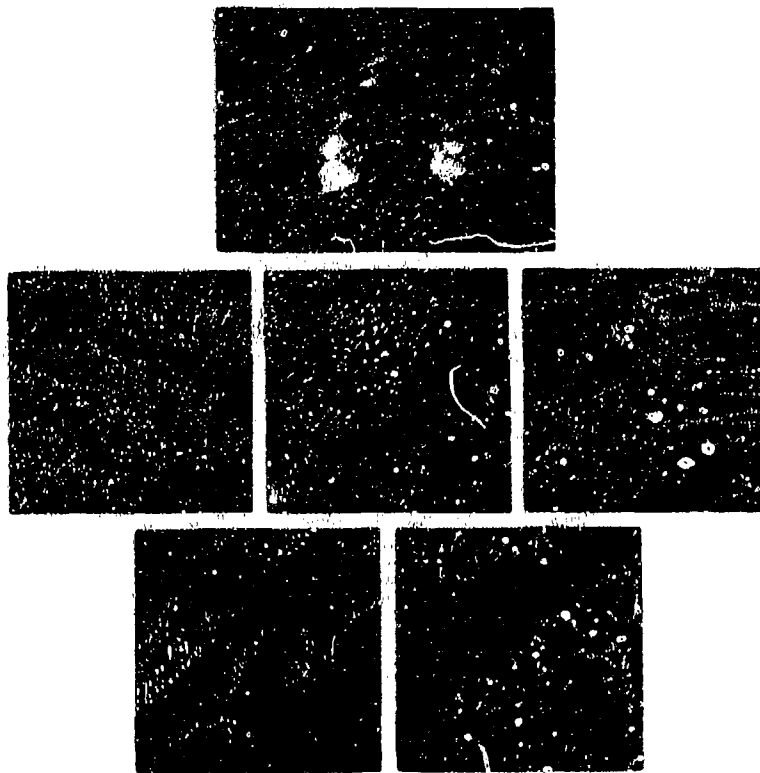



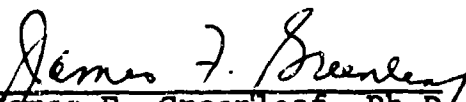
Figure 11. Changes in regional lung volume, obtained from reconstructed cross sections of unit thickness of the intact right and left lung of a living dog, at five different levels during the respiratory cycle. The cross sections obtained as described in Figure 10 were also used to construct this figure and are presented in the same format.


Surrounding the anteroposterior view of the canine thorax with a brightened horizontal line superimposed at each of the five levels at which cross sections were obtained are plots of relative regional lung volume (normalized to the maximal regional volume observed - at level 4) versus relative tidal volume (percent of maximal tidal volume) for the right (R) and left (L) lung at each specified lung level. The inspiratory (I) and expiratory (E) phases of the respiratory cycle are indicated.

Summary

It is now clear that the pulmonary parenchymal marker and three-dimensional reconstruction techniques described herein will add significant new information to our understanding of dynamic regional stress-strain relationships throughout the lung and will thereby provide the methodology to study the effects on regional lung function of alterations in these parameters induced by changes in the gravitational-inertial force environment. Since the pulmonary system is the most susceptible system of the body to the influence of gravity, these studies are necessary to determine means of reducing or alleviating the potentially harmful effects of increased gravitational-inertial force environments.


Earl H. Wood, M.D., Ph.D.
Project Director


James F. Greenleaf, Ph.D.
Co-Principal Investigator


Peter A. Chevalier, Ph.D.
Co-Principal Investigator

August 28, 1974

References

1. Smith, H. C., J. F. Greenleaf, E. H. Wood, D. J. Sass and A. A. Bove:
Measurement of regional pulmonary parenchymal movement in dogs.
J Appl Physiol 34:544-547, 1973.
2. Sturm, R. E., E. L. Ritman, R. J. Hansen and E. H. Wood:
Recording of multichannel analog data and video images on the same videotape or disc.
J Appl Physiol 36:761- 764, 1974.
3. West, J. B., and F. L. Matthews:
Stresses, strains and surface pressures in the lung caused by its weight.
J Appl Physiol 32:332-345, 1972.
4. Johnson, S. A., R. A. Robb, J. F. Greenleaf, E. L. Ritman, S. L. Lee, G. T. Herman, R. E. Sturm, and E. H. Wood:
The problem of accurate measurement of left ventricular shape and dimensions from multiplane roentgenographic data.
Eur J Cardiol 1/3, 241-258, 1974.
5. Gordon, R., and G. T. Herman:
Reconstruction of pictures from their projections.
Communications Association Computer Machines, 14, 1971.
6. Gordon, R., and G. T. Herman:
Three-dimensional reconstruction from projections: A review of algorithms.
Int Rev Cytol 38:111-151, 1974.

MANUSCRIPTS AND ABSTRACTS PUBLISHED

1. Bourgeois, M. J., B. K. Gilbert, D. E. Donald, and E. H. Wood:
Characteristics of aortic diastolic pressure decay
with application to the continuous monitoring of changes
in peripheral vascular resistance.
Circ Res 35:56-66 (July) 1974.
2. Johnson, S. A., R. A. Robb, J. F. Greenleaf, E. L. Ritman,
S. L. Lee, G. T. Herman, R. E. Sturm, and E. H. Wood:
The problem of accurate measurement of left ventricular
shape and dimensions from multiplane roentgenographic
data.
Eur J Cardiol 1/3, 241-258, 1974.
3. Sturm, R. E., E. L. Ritman, R. J. Hansen, and E. H. Wood:
Recording of multichannel analog data and video images
on the same video tape or disc.
J Appl Physiol 36:761-764, 1974.
4. Yipintsoi, T., and E. H. Wood:
The history of circulatory indicator dilution.
In Dye Curves. The Theory and Practice of Indicator
Dilution (Dr. Dennis A. Bloomfield, editor) University
Park Press, Baltimore, 1974, pp 1-19.
5. Bursch, J. H., E. L. Ritman, E. H. Wood, and R. E. Sturm:
Roentgen videodensitometry.
Ibid. pp 313-333.
6. Greenleaf, J. F., S. A. Johnson, S. L. Lee, G. T. Herman,
and E. H. Wood:
Algebraic reconstruction of spatial distributions of
acoustic absorption within tissue from their two-dimensional
acoustic projections.
In Acoustical Holography. Volume 5. (Philip S. Green,
editor) Plenum Press, New York, 1974, pp 591-603.
7. Chevalier, P. A., J. F. Greenleaf, R. A. Robb, and E. H. Wood:
Biplane videoroentgenographic analysis of dynamic regional
lung strains in dogs.
Physiologist 17:195 (August) 1974. Abstract
8. Greenleaf, J. F., E. L. Ritman, E. H. Wood, R. A. Robb, and
S. A. Johnson:
Dynamic computer-generated displays of data from biplane
roentgen angiography for study of the left ventricle.
Ann Biomed Eng 2, 90-105, 1974.
9. Robb, R. A., E. L. Ritman, J. F. Greenleaf, S. A. Johnson,
and E. H. Wood:
Three-dimensional reconstruction of dynamic in-vivo
heart by multiplanar x-ray videodensitometry.
Fed Proc 33:965 (March) 1974. Abstract

10. Wood, E. H., D. Allen, and B. Jewell:
Preponderance of postsystolic period in the positive
inotropic effects of increases in $[Ca^{++}]_O$.
Fed Proc 33:552 (March) 1974. Abstract
11. Ritman, E. L., S. A. Johnson, R. E. Sturm, and E. H. Wood:
Limitations and improvement of the dynamic response of
television cameras for ventriculography.
Proc Symposium on Human Left Ventricular
Performance, International Society of Cardiology,
Bordeaux, France, September 10-11, 1973, p 13. Abstract
12. Sass, D. J., A. C. Nolan, and E. H. Wood:
Digital computer analysis of circulatory and respiratory
pressures in water-immersed dogs breathing liquid in
force environments of 1 and 7Gy.
Aerosp Med 45:1-11 (January) 1974.
13. Allen, D. G., B. R. Jewell and E. H. Wood:
The rested state contraction and action potential of cat
papillary muscle.
Proc Physiological Society, December 14-15,
1973, pp 29-31. Abstract
14. Dumesnil, J. G., E. L. Ritman, R. L. Frye, G. D. Davis,
G. T. Gau, R. E. Sturm, and E. H. Wood:
Regional left ventricular wall dynamics before and after
the administration of oral nitroglycerine.
Circulation 48:4:410 (October) 1973. Abstract
15. Robb, R. A., S. A. Johnson, J. F. Greenleaf, M. A. Wondrow,
and E. H. Wood:
An operator-interactive, computer-controlled system for
high-fidelity digitization and analysis of biomedical images.
Proc Soc Photo-optical Instrumen-
tation Engineers, August 27-29, 1973, Volume 40, pp 11-26.
16. Ritman, E. L., R. E. Sturm, and E. H. Wood:
Biplane roentgen videometric system for dynamic (60/sec)
studies of the shape and size of circulatory structures,
particularly the left ventricle.
Am J Cardiol Vol 32, No 2, 180-187 (August) 1973.
17. Smith, H. C., R. E. Sturm, and E. H. Wood:
Videodensitometric system for measurement of vessel blood
flow, particularly in the coronary arteries, in man.
Am J Cardiol Vol 32, No 2, pp 144-150 (August) 1973.
18. Tsakiris, A. G., R. E. Sturm, and E. H. Wood:
Experimental studies on the mechanisms of closure of
cardiac valves with use of roentgen videodensitometry.
Am J Cardiol Vol 32, No 2, pp 136-143 (August) 1973.

19. Tsuiki, K., E. L. Ritman, D. E. Donald, R. E. Sturm, and E. H. Wood:
Videometric determination of wall dynamics in a working isolated canine left ventricle.
Physiologist 16:473 (August) 1973. Abstract
20. Ritman, E. L., D. E. Donald, K. Tsuiki, R. E. Sturm, and E. H. Wood:
Videometric determination of dynamic regional shape and dimensions of an isolated working canine left ventricle.
Physiologist 16:434 (August) 1973. Abstract
21. Sass, D. J., R. A. VanDyke, E. H. Wood, S. A. Johnson, and P. E. Didisheim:
Gas embolism due to intravenous FC 80 liquid fluorocarbon. Aersp Med Assn Preprints, 1973 Annual Scientific Meeting, Las Vegas, Nevada, May 7-10, 1973, pp 42-43. Abstract
22. Sass, D. J., E. H. Wood, J. F. Greenleaf, E. L. Ritman, and H. C. Smith:
Effects of breathing liquid fluorocarbons on regional differences in pleural pressures and other physiological parameters.
SAM-TR-72-15, USAF School of Aerospace Medicine, Brooks Air Force Base, Texas, pp 1-173, December 1972.
23. Miyazawa, K., H. C. Smith, E. H. Wood, and A. A. Bove:
Roentgen videodensitometric determination of left-to-right shunts in experimental ventricular septal defect.
Am J Cardiol 31:627-634 (May) 1973.
24. Ritman, E. L., S. A. Johnson, R. E. Sturm, and E. H. Wood:
The television camera in dynamic videoangiography.
Radiology 107:417-427 (May) 1973.
25. Smith, H. C., J. F. Greenleaf, E. H. Wood, D. J. Sass, and A. A. Bove:
Measurement of regional pulmonary parenchymal movement in dogs.
J Appl Physiol 34:544-547 (April) 1973.
26. Greenleaf, J. F., E. L. Ritman, E. H. Wood, R. L. Frye, R. A. Robb, and S. A. Johnson:
Dynamic computer-generated displays for study of the human left ventricle.
Proc Soc of Photo-optical Instrumentation Engineers, Seminar, Developments in Electronic Imaging Techniques, October 16-17, 1972, San Mateo, California, Vol 32:111-122, 1973.

27. Dumesnil, J. G., E. L. Ritman, R. L. Frye, G. T. Gau, B. D. Rutherford, G. D. Davis, and E. H. Wood:
Regional left ventricular wall dynamics by roentgen videometry.
J Lab Clin Med 21:3:415 (April) 1973. Abstract
28. Bourgeois, M. J., B. K. Gilbert, and E. H. Wood:
Analysis of stroke volume via the aortic pressure pulse contour.
Fed Proc 32:331 (March) 1973. Abstract
29. Ritman, E. L., S. A. Johnson, R. E. Sturm, and E. H. Wood:
Distortion of dynamic roentgen angiographic images by the video camera.
Proc Biomedical Engineering Society, 3rd Annual Meeting, Maryland, 1972, p 69. Abstract
30. von Bernuth, G., A. G. Tsakiris, and E. H. Wood:
Quantitation of experimental aortic regurgitation by roentgen videodensitometry.
Am J Cardiol 31:265-272 (February) 1973.
31. Greenleaf, J. F., S. A. Johnson, and E. H. Wood:
Comparison of ultrasound cardiography with biplane angiography.
Progress report to the U.S. Air Force on Contract AF F44620-71-C0069, July, 1973.
32. Greenleaf, J. F., and E. H. Wood:
Protection of the cardiopulmonary systems against the injurious effects of acceleration.
Annual Report to the U.S. Air Force, Washington, D.C., September 1, 1973.

PAPERS IN PRESS

1. Johnson, S. A., R. A. Robb, J. F. Greenleaf, E. L. Ritman, B. K. Gilbert, M. T. Storma, J. D. Sjostrand, D. E. Donald, G. T. Herman, R. E. Sturm, and E. H. Wood:
Dynamic three-dimensional reconstruction of beating heart and lungs from multiplanar roentgen-television images.
Mayo Clin Proc
2. Robb, R. A., J. F. Greenleaf, E. L. Ritman, S. A. Johnson, J. Sjostrand, G. T. Herman, and E. H. Wood:
Three-dimensional visualization of the intact thorax and contents: A technique for cross-section reconstruction from multiplanar x-ray views.
Comp Biomed Res

3. Ritman, E. L., J. H. Bursch, H. C. Smith, R. E. Sturm,
and E. H. Wood:
Roentgen videodensitometry and videoscanning densitometry
application to the cardiovascular system.
Monograph on New Diagnostic Pararadiologic Technology,
Dr. Manuel Viamonte, Jr., editor.
4. Ritman, E. L., R. L. Frye, G. D. Davis, B. D. Rutherford,
G. T. Gau, and R. E. Sturm:
A biplane roentgen videometry system for dynamic studies
of the shape and size of the human left ventricle.
Circulation
5. Greenleaf, J. F., E. L. Ritman, D. J. Sass, and E. H. Wood:
Spatial distribution of pulmonary blood flow in dogs in
left decubitus position.
J Appl Physiol
6. Wood, E. H., E. L. Ritman, J. F. Greenleaf, R. A. Robb,
S. A. Johnson, and R. E. Sturm:
The problem of accurate measurement of the shape and
dimensions of the left ventricle from multiplane
roentgenographic data.
Proc XII International Congress of Radiology
Madrid, Spain (October) 1973.
7. Pao, Y. C., E. L. Ritman, and E. H. Wood:
Finite element analysis of left ventricular myocardial
stresses.
J Biomech
8. Dumesnil, J. G., E. L. Ritman, R. L. Frye, G. D. Davis,
G. T. Gau, B. D. Rutherford, R. E. Sturm, and E. H. Wood:
Quantitative determination of regional left ventricular
wall dynamics by roentgen videometry.
Circulation
9. Ritman, E. L., R. Frye, J. Dumesnil, G. Davis, R. Sturm, and
E. H. Wood:
Roentgen videometric determination on the left ventricular
shape, dimensions and wall dynamics.
Proc Association of University Radiologist Seminar
Myocardial Circulation Imaging (and Ventricular
Function Imaging), Palm Springs, California, January
24-26, 1974.
10. Bursch, J. H., E. L. Ritman, R. E. Sturm, and E. H. Wood:
Videodensitometric determination of left ventricular
ejection and filling characteristics.
J Appl Physiol

11. Greenleaf, J. F., H. C. Smith, E. H. Wood, D. J. Sass,
and A. A. Bove:
Effect of changes in magnitude of force environment on
regional pulmonary displacements and volumes of dogs in
left decubitus position.
J Appl Physiol
12. Pao, Y. C., R. A. Robb, and E. L. Ritman:
Plain-strain finite-element analysis of reconstructed
left ventricular cross sections.
J Appl Physiol (to be submitted)
13. Ritman, E. L.:
Left ventricular function and myocardial contractility:
Analysis by roentgen video-angiographic techniques.
Mayo Clinic Proc
14. Sass, D. J., R. A. Van Dyke, E. H. Wood, S. A. Johnson,
and Paul Didisheim:
Gas embolism due to intravenous FC 80 liquid fluorocarbon.
J Appl Physiol